Biorobotic Locomotion: Biped Humanoid Walking using Optimal Control

A Thesis
Presented to
The Academic Faculty

by

Malavika Bindhi

In Partial Fulfillment
of the Requirements for the Degree
Bachelor of Science in Electrical Engineering with the Research Option in the
School of Electrical and Computer Engineering

Georgia Institute of Technology
May, 2017

Biorobotic Locomotion: Biped Humanoid Walking using Optimal Control

Approved by:

Dr. Patricio Vela , Advisor
School of Electrical and Computer Engineering
Georgia Institute of Technology

Dr. Erik Verriest
School of Electrical and Computer Engineering
Georgia Institute of Technology

Date Approved: 05/05/2017

[To the students of the Georgia Institute of Technology]

TABLE OF CONTENTS

SUMMARY

This paper explores the use of optimal control for quasi-static bipedal walking trajectory synthesis. Optimal control differs from the traditional method of inverse kinematics used for generating trajectories. On setting up an optimal control problem and solving it, a set of joint angle trajectories for executing a portion of the gait can be synthesized using the forward kinematic description, as opposed to the method of inverse kinematics. Although optimal control solution requires the same computational processing, the advantage is the simplification of problem set up procedure. This research aims at developing a quasi-static walking gait for a humanoid by defining a set of optimal control problems with constraints and costs defined as functions of joint angles. OPTRAGEN, a Matlab toolbox, is used to convert the optimal control problem to a non-linear problem which is then solved by a numerical optimization program. The goal is to generate a planar walking gait by setting up an optimal control problem that minimizes the change in joint angles while keeping the body stable. The generated planar gait was tested on the physical robot. On completion of this, the same methods were also used to generate trajectories for a 3-Dimensional quasi-static walking gait. .

CHAPTER 1

INTRODUCTION

One established area of research in the field of robotics is Bio-robotic Locomotion, which is a field that tries to mimic the locomotion of biological creatures. Examples of such robots include quadrupeds that are four-legged and mimic cats or dogs, bipeds which are two-legged similar to humans, and hexapods which are eight-legged like spiders. In the more specific case of a humanoid, significant effort has been put into achieving the ability of the humanoid to walk in a natural manner. While there has been a focus on imitation of the human motion to develop the movements of a humanoid, the methods used differ. Over the past years, research efforts have solved the problems of stability control, static walking, and highly efficient dynamic walking for humanoids using the center of mass and zero moment point calculated for the humanoid [1-2]. Algorithms have also been developed to map the human motion to humanoid by integrating stability control of humanoid with motion capture of humans [3]. More recently, there has been a focus on developing the ability to walk on uneven surfaces such as rocks or ascending and descending of stairs [4]. Some of the natural actions performed by humans, for example walking around a building, could be mimicked by humanoids. Similar to humans, the humanoids must be able to autonomously decide their path while moving around in different environments. Many approaches have been utilized to move in this direction, some of them being vision-based humanoid footstep planning and sample-based planning [5]. Since path planning is a relatively new track, ongoing

research aims at identifying the best solution to the question of natural movement of humanoids.

Optimal control has been used earlier to generate walking gaits for humanoids [23]. This research project is aimed at developing a simplified method of generating walking gaits for biped quasi-static walking through optimal control. Statically stable walking is defined as an optimal control problem using the forward kinematics of the robot to define constraints while the squared norm of the joint angle velocity is defined as the cost that needs to be minimized. The aim is to use Optragen [24], a Matlab toolbox that converts optimal control problems to non-linear problems. Then the non-linear problem is solved by a numerical optimization program. Thus here we explore multiple optimal control problems that can be solved easily by Optragen and a solver in order to generate walking gaits for a humanoid. The initial steps involve modeling of forward kinematics for a Bioloid GP humanoid (shown in Figure 1). Following this, an optimal control problem is set up as a set of constraints and costs from which the trajectories can then be generated. As opposed to some of the

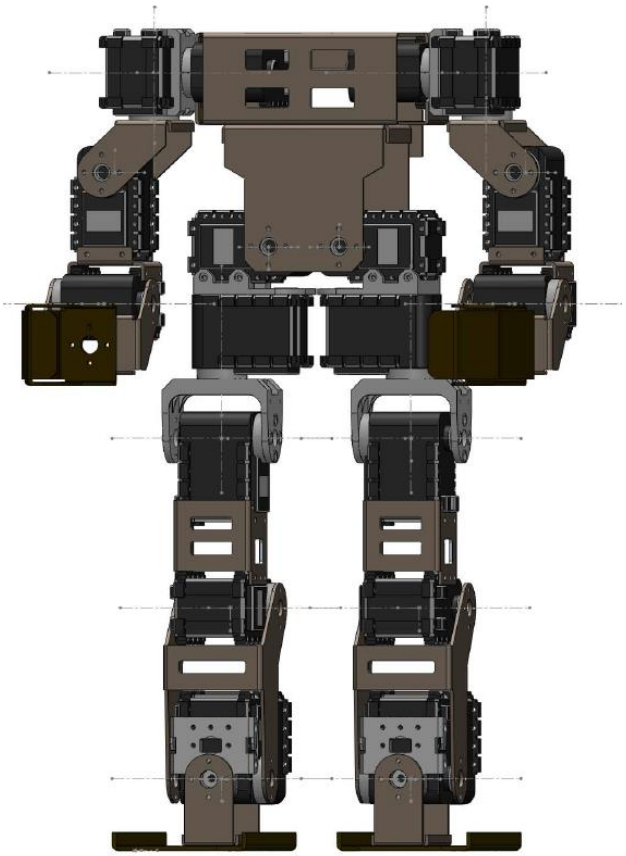

Figure 1: Manny, the Humanoid.

traditional methods of generating trajectories using inverse kinematics, this method simplifies the process as an optimal control problem setup can solve for a set of joint angles that can perform a part of a gait in one step. The focus of this thesis will be to generate trajectories for a planar model of the biped but we also generate trajectories for a 3D model.

Literature Review

Over the past several decades, researchers have had an increased interest in humanoid robots and there are several reasons for this interest [6]. One of them is the capability of humanoids, with their anthropomorphic structure, to traverse man-made environments with varying structures like stairs, or other obstacles. It would be difficult for a wheeled robot to accomplish such a task. The aim of developing a humanoid robot is to allow these robots to handle dangerous environments, like firefighting, radioactive areas, or construction sites, thereby removing humans from danger. In order to reach this target, it is imperative for the humanoids to be able to move around the man-made environments in a manner very similar to humans, being able to decide their own path, and to avoid obstacles. The following sections summarize some of the relevant developments in the field.

I. Formulation of Variables:

Two of the most commonly used parameters to model the kinematics of a humanoid are Center of Mass and Zero Moment Point. Cotton et al. propose the use of Statically Equivalent Serial Chain (SESC) modeling in order to find the center of mass of the humanoid [7]. The algorithm uses only mechanical parameters, i.e. SESC is modeled based on the known parameters of mass of each link, center of mass of each link, and

location of each joint relative to the previous joint. Hence, using this algorithm allows for efficient calculation of the center of mass for humanoid with any Degrees of Freedom (DOF) based on the original reference point. Kwon et al. suggest that a closed loop method to find the center of mass would be more accurate than an open loop method [8]. A discrete Kalman Filter is used to achieve this. The center of mass is initially estimated using the joint angles and link parameters in a traditional method. A feedback is used to modify this center of mass according to the error in the center of mass measured. Therefore, their model provides a more accurate real-time measurement of center of mass. By combining the SESC model and closed loop calculation method, the measurement of center of mass would be efficient and accurate.

To achieve statically stable walking, the projection of the center of mass of the humanoid must lie within the support polygon [9]. The limitation of this kind of walking model is that it allows only slow speeds. At the same time, a dynamically stable walking model permits the center of mass to lie outside the support polygon through the control of the position based on the Zero Moment Point (ZMP). ZMP is a point on the surface of contact where a reaction force can act as the sum of all forces acting on the surface. If the ZMP lies within the support polygon, the motion is said to be dynamically stable, and the robot does not tip over, even if the center of mass lies outside the support polygon [6]. Both of these parameters, together form the base of the linear inverted pendulum model (LIPM).

In [11], Grizzle et al. developed asymptotically stable walking for biped robots by dividing the model into two parts; the swing phase model, and the impact model. The swing phase model is valid when one leg is off the ground, and the impact model is valid

when the leg touches the ground. Then the method of Poincaré sections is used to develop asymptotic stability of walking cycle. The formulation of the biped as a nonlinear system with impact effects helps in reducing the complexity of the Poincaré map. Ames et al. use human walking data to model the parameters of humanoid robotic controllers subject to the constraints of partial hybrid zero dynamics [12]. Applying this constraint allowed the generation of parameters for robotic control that ensures the existence of a stable walking gait.

II. Walking Pattern Planning for Humanoids:

Many proposed methods for generating walking patterns use the linear inverted pendulum model (LIPM). All of these models aim at developing stable walking gaits. One of the early methods was proposed in [13], where Fourier series was used to generate a stable walking pattern. The method uses iterative calculation, hence is not efficient in a real-time environment. Kajita et al. developed a three-dimensional LIPM for generating walking pattern for humanoid where limited parameters were used to model the walking pattern. The model is defined in terms of second order differential equations [15]. Yi et al. considered the use of fictitious zero moment point (FZMP) method to enable stability of humanoid, while being exposed to environmental perturbations [2]. Czarnetzki et al. propose the use of a feedback sensor based control system for dynamic walking of a humanoid robot [9]. The system consists of a controller, which is an online path planner, and an observer, which consists of sensors providing feedback to the controller. Such a system will be able to handle the irregularities present in the real world and prevents the humanoid from tipping over in case of unexpected disturbances.

III. Optimal Control based Trajectory Generation:

All of the above methods were derived to achieve the stability in the walking pattern of humanoid. They aimed at maintaining stability in walking even in the cases of uneven surfaces, or sudden disturbances. Other than the above-mentioned methods, there have been many more proposed methods to achieve the same target with more robustness [16-20]. Optimal control based trajectory generation is also a proposed method to achieve stable walking gaits as shown by Koch et. al [23]. An optimal control Matlab toolbox called Optragen, developed by Raktim Bhattacharya, can be used for numerically solving optimal control problems [24]. Optragen takes in the optimal control problem, set up in the form of constraints and costs, and gives the output as a non-linear problem consisting of a constraint function and a cost function. Any non-linear problem solver can then be used to solve this. SNOPT (Sparse Nonlinear OPTimizer) is a non-linear problem solver that can take in the results from Optragen and solve for the final trajectory values [25]. This research aims at developing quasi-static walking gait for a humanoid by setting up multiple optimal control problems that are defined in terms of the joint angles. Then Optragen and a numerical optimization program are used to solve for the joint trajectories. The main focus will be on setting up of the optimal control problems to successfully generate joint trajectories.

CHAPTER 2

METHODS AND MATERIALS

This chapter describes the methods used to develop a walking gait for a humanoid robot. The chapter first describes the method by which the robot's computer-based model was generated, which was then used in order to develop the gait. Following the description of the model, the chapter also describes some of the most crucial calculations such as center of mass and support polygon. The methods used for these calculations have been discussed in detail in chapter 1. The section IV of this chapter describes the use of optimal control to generate a planar walking gait. The last section extends the gait synthesis to a 3D model.

I. Measurements and setting up of coordinate frames

The first task involved assigning each joint with a reference coordinate frame, which is described in terms of a translation and a rotation relative to the frame of the previous joint. There are 22 joints in total for the humanoid, with each leg having 6 joints and each arm having 5 joints. Figure 2 shows the assignments of coordinate frames for joints on the left leg and left arm of the humanoid. The right leg and arm assignments are similar to the assignments on the left side of the humanoid. In addition to these coordinate reference frames, a few other frames were also added. These include the torso reference frame, and a reference frame at the center of the base of each foot.

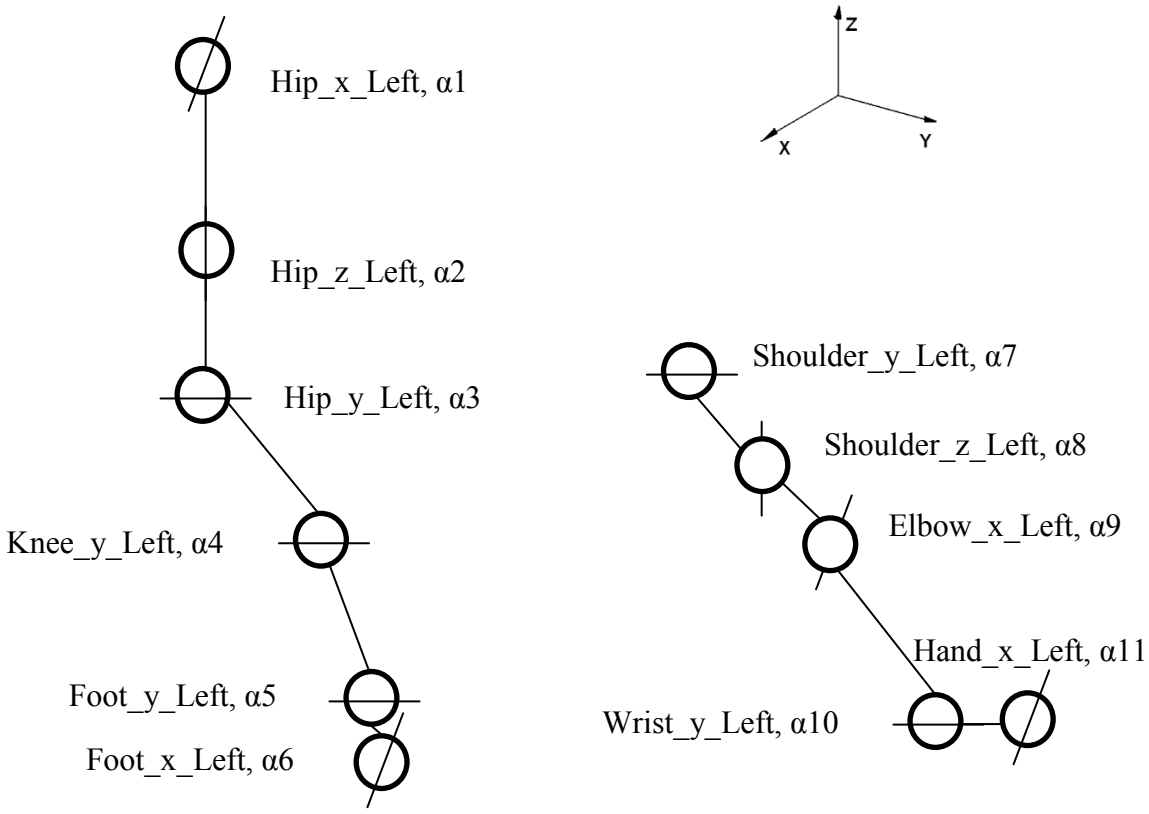

Each joint is defined as (A_B_C, D) where A is the location of the joint, B is the axis of rotation, C is the side of the body, and D is name of the joint angle. The right side of the body follows the same structure and joint angles from α12 –α22 account for the these angles in the same order.

Figure 2: Description of Coordinate Frames for Joints on Left Side of Humanoid.

Transformation matrices were set up for each reference frame and the model is defined as a kinematic chain. The translation measurements from one joint to next were made by using the measurement tools available for the CAD model of the robot. The measurement is made from the origin of one coordinate frame to that of the next coordinate frame. The rotation matrices are defined according to the axis about which the joints rotate. Each link's mass was also measured using the CAD model available.

II. Center of Mass for the Humanoid

Center of mass for the humanoid was calculated by using the traditional method. It is defined as

$$CoM = \sum_{i=frame}^{n} \frac{m_i c_i}{M} g_i^{ref}$$

where m_i is mass of the i^{th} link, c_i is the center of mass of the i^{th} link, M is the total mass of the humanoid, and g_i^{ref} is the transformation matrix from reference coordinate frame to i^{th} coordinate frame. Defining a link as the rigid body between two joints, the mass and center of mass of each link was measured using the Mass Properties tools in the CAD model. Then by applying the above-mentioned formula, the center of mass of the humanoid with respect to the torso frame, left foot frame and right foot frame were calculated.

III. Support Polygon

Static walking assumes that a robot is statically stable at all times. This means, if the robot were to stop at any point during the motion, it will remain upright. Static stability is attained by having the robot's center of mass projected on to its support polygon. For a robot walking on a flat surface, the support polygon is the convex hull of its foot or feet (depending on how many are on the ground). For planar case, the projection of the x component of center of mass must lie within an interval. For the 3D case, the x and y components of center of mass must lie within the support polygon.

IV. Biped Walking Gait Development

The walking gait for the robot is achieved by using the optimal control software package called Optragen. Optragen is a MATLAB toolbox which converts an optimal control problem to a non-linear control problem which is then solved by SNOPT. To obtain a quasi-static walking gait as close to humans as possible, a series of steps to be executed were developed. The main idea behind this is that once the robot has reached a stance where one leg is in front of the other leg, walking is just a repetitive cycle of events. For this purpose, the gait generated was divided into 7 steps, which includes a pre-cyclic stage, left leg gait and right leg gait. The pre-cyclic stage sets the right leg ahead of the left leg after which left leg gait and right leg gait are alternated. Table 1 shows in detail the location of each foot at the end of these cycles along with the region in which x projection of the center of mass of the body lies. To help visualize this better, Figure 3 shows that change in the robot's body positions over these seven stages. The figure also shows the center of mass positions at the end of these stages.

Table 1: Detailed Description of Foot Position during the Walking Gait

Part of Walking Gait	Left Foot Position (x,z)	Right Foot Position (x,z)	Center of Mass Location
Initial	(0,0)	(0,0)	Over Both Feet
Pre-Cycle Stage	(-2,0)	(0,0)	Over Right Foot
Left Cycle Stage 1	(0,1)	(0,0)	Over Right Foot
Left Cycle Stage 2	(2,0)	(0,0)	Over Right Foot
Left Cycle Stage 3	(2,0)	(0,0)	Over Left Foot
Right Cycle Stage 1	(2,0)	(2,1)	Over Left Foot
Right Cycle Stage 2	(2,0)	(4,0)	Over Left Foot
Right Cycle Stage 3	(2,0)	(4,0)	Over Right Foot

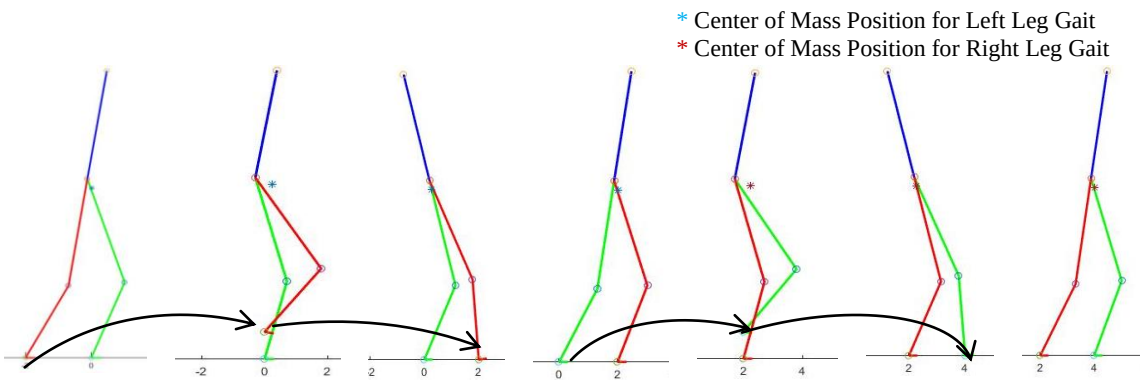

Figure 3: Walking gait displayed using planar visual model.

Following the description shown in this table, the optimal control problem was set up to have constraints that allow for each leg to reach the required position while minimizing the change in joint angles and maintaining stability. The constraints used for each stage is detailed in Tables 2, 3, and 4. The joint angles on the left leg and right leg are defined as α_L and α_R respectively where α stands for joint angles as defined in Figure 2. X_{LF}^{RF} is the x coordinate of position of left foot base frame with respect to right foot base frame whereas Z_{LF}^{RF} is the z coordinate. X_{COM}^{RF} is the projection of center of mass along x axis with respect to right foot base frame. The first constraint is the constraint on the foot position of left leg throughout the trajectory while the second constraint is the final position to be reached. The center of mass constraint maintains the stability of the body throughout the trajectory and the fourth constraint maintains the orientation. Due to the anthropomorphic structure of the robot, the knee joint can only move in one direction, specified by the fifth joint. Left Cycle Stage 1 and Left Cycle Stage 2 constraints are similar in nature. For Left Cycle Stage 3, since the feet remain stationary, there is a no

requirement of separate trajectory and final position constraints. For all of these control problems, the cost function is defined as

$$Cost = \sum_{i \in I_p} \left\| \dot{\alpha} \right\|^2$$

$$I_p = \{3, 4, 5, 14, 15, 16\}$$

where α are joint angles as defined in Figure 2. For the case of planar walking, only the joint angles that rotate about the y axis are used to set up the optimal control problem. Therefore, all the constraints are defined in terms of variables that vary along the x and z axes.

The synthesized trajectory was then implemented on the physical robot. Since a planar walking gait was developed, the physical implementation on the robot requires an external support that prevents the body from tipping along the direction that is not controlled (in this case, about y axis). A boom was designed to allow the robot moment about x and z axes while providing support about the y axis. The boom allows the robot to walk along a circular path.

Table 2: Left Cycle Stage 1 Control Problem Definition

Description	Equations
1) Foot Position Trajectory Constraint	$0 \leq Z_{LF}^{RF}(\alpha_L, \alpha_R) \leq 1$ $0.5^2 \leq (X_{LF}^{RF}(\alpha_L, \alpha_R) + 1.4)^2 + (Z_{LF}^{RF}(\alpha_L, \alpha_R) + 0.2)^2 \leq \infty$
2) Final Foot Position	$X_{LF}^{RF}(\alpha_L, \alpha_R) = 0$ $Z_{LF}^{RF}(\alpha_L, \alpha_R) = 1$

3) Center of Mass Constraints	$-0.01 \leq X_{COM}^{RF}(\alpha) \leq 1.2$
4) Constraint to maintain orientation	$\sum_{i=3}^{5} \alpha_i = 0$
5) Knee Joint Constraint	$\alpha 4 \geq 0;$

Table 3: Left Cycle Stage 2 Control Problem Definition

Description	Equations
1) Foot Position Trajectory Constraint	$0 \leq X_{LF}^{RF}(\alpha_L, \alpha_R) \leq 2$ $0 \leq Z_{LF}^{RF}(\alpha_L, \alpha_R) \leq 1$
2) Final Foot Position	$X_{LF}^{RF}(\alpha_L, \alpha_R) = 2$ $Z_{LF}^{RF}(\alpha_L, \alpha_R) = 0$
3) Center of Mass Constraints	$0.2 \leq X_{COM}^{RF}(\alpha) \leq 1.2$
4) Constraint to maintain orientation	$\sum_{i=3}^{5} \alpha_i = 0$, $\sum_{i=14}^{16} \alpha_i = 0$
5) Knee Joint Constraint	$\alpha 4 \geq 0;$ $\alpha 15 \geq 0$

Table 4: Left Cycle Stage 3 Control Problem Definition

Description	Equations

1) Foot Position Trajectory Constraint	$X_{LF}^{RF}(\alpha_L, \alpha_R) = 2$ $Z_{LF}^{RF}(\alpha_L, \alpha_R) = 0$
2) Center of Mass Trajectory Constraint	$1 \leq X_{COM}^{RF}(\alpha) \leq 3.2$
3) Center of Mass Final Constraint	$2.8 \leq X_{COM}^{RF}(\alpha) \leq 3.2$
4) Constraint to maintain orientation	$\sum_{i=3}^{5} \alpha_i = 0$, $\sum_{i=14}^{16} \alpha_i = 0$
5) Knee Joint Constraint	$\alpha 4 \geq 0; \quad \alpha 15 \geq 0$

V. 3D Walking Gait:

On completion of the planar walking gait, the next stage of research is to generate the walking gait for a 3D model of the humanoid. The same methods are used as before with few changes. One major change would be the solver that is used. SNOPT's open source version has an upper bound on the number of variables that can be used to set up the optimal control problem. Hence, the maximum number of joints that can be controlled at a time using SNOPT would be 7. In order to generate a 3D walking gait for this humanoid, at least 10 joints need to be controlled at the same time. Therefore, a new solver called IPOPT is used for generating 3D walking gaits. IPOPT can solve for all 10 joint trajectories at the same time.

With respect to setting up the optimal control problem, few new constraints are required to maintain stability of the body. The projection of the center of mass of the body along both the x and y axes must lie within the support polygon. Also, there is a need of an additional constraint on the position of the base of the foot along the y direction, in order to avoid any abnormal movements. Addition of these constraints would then be able to produce a 3D quasi-static walking gait for the humanoid. The constraints used to define the optimal control problem for each stage are defined in detail in Tables 5, 6, and 7. All variables defined in the previous section hold true here and the constraints are defined in the same manner as well. One of the new variables is Y_{LF}^{RF}, the y coordinate of the position of the left foot base frame with respect to the right foot base frame. Y_{COM}^{RF} is the projection of center of mass along y axis with respect to the right foot base frame. The cost function for each control problem is defined as:

$$Cost = \sum_{i \in I_p} \left\| \dot{\tilde{\alpha}} \right\|^2$$

$$I_p = \{1,3,4,5,6,12,14,15,16,17\}$$

where α is the set of joint angles defined in Figure 2. For 3D walking gait, three angles that rotate about the y axis and two angles that rotate about the x axis on each leg is used to define all the variables.

Table 5: 3D Left Cycle Stage 1 Control Problem Definition

Description	Equations

1) Final Foot Position	$X_{LF}^{RF}(\alpha_L, \alpha_R) = 0$ $Y_{LF}^{RF}(\alpha_L, \alpha_R) = 5$ $Z_{LF}^{RF}(\alpha_L, \alpha_R) = 1$
2) Center of Mass Constraints	$-0.4 \leq X_{COM}^{RF}(\alpha) \leq 1.2$ $-0.3 \leq Y_{COM}^{RF}(\alpha) \leq 0.8$
3) Constraint to maintain orientation	$\sum_{i=3}^{5} \alpha_i = 0$, $\sum_{i=14}^{16} \alpha_i = 0$, $\alpha 1 + \alpha 6 = 0$, $\alpha 12 + \alpha 17 = 0$
4) Knee Joint Constraint	$\alpha 4 \geq 0$; $\alpha 15 \geq 0$

Table 6: 3D Left Cycle Stage 2 Control Problem Definition

Description	Equations
1) Foot Position Trajectory Constraint	$0 \leq Z_{LF}^{RF}(\alpha_L, \alpha_R) \leq 1$
2) Final Foot Position	$X_{LF}^{RF}(\alpha_L, \alpha_R) = 2$ $Y_{LF}^{RF}(\alpha_L, \alpha_R) = 4$ $Z_{LF}^{RF}(\alpha_L, \alpha_R) = 0$
3) Center of Mass Constraints	$-0.4 \leq X_{COM}^{RF}(\alpha) \leq 1.2$ $0.7 \leq Y_{COM}^{RF}(\alpha) \leq 1$
4) Constraint to maintain	$\sum_{i=3}^{5} \alpha_i = 0$, $\sum_{i=14}^{16} \alpha_i = 0$, $\alpha 1 + \alpha 6 = 0$, $\alpha 12 + \alpha 17 = 0$

orientation	
5) Knee Joint Constraint	$\alpha 4 \geq 0;\ \alpha 15 \geq 0$

Table 7: 3D Left Cycle Stage 3 Control Problem Definition

Description	Equations
1) Foot Position Trajectory Constraint	$X_{LF}^{RF}(\alpha_L, \alpha_R) = 2$ $Z_{LF}^{RF}(\alpha_L, \alpha_R) = 0$
2) Center of Mass Trajectory Constraint	$1 \leq X_{COM}^{RF}(\alpha) \leq 3.2$ $1 \leq Y_{COM}^{RF}(\alpha) \leq 2$
3) Center of Mass Final Constraint	$2.8 \leq X_{COM}^{RF}(\alpha) \leq 3.2$ $1.6 \leq Y_{COM}^{RF}(\alpha) \leq 2$
4) Constraint to maintain orientation	$\sum_{i=3}^{5} \alpha_i = 0$, $\sum_{i=14}^{16} \alpha_i = 0,\ \alpha 1 + \alpha 6 = 0,\ \alpha 12 + \alpha 17 = 0$
5) Knee Joint Constraint	$\alpha 4 \geq 0;\ \alpha 15 \geq 0$

CHAPTER 3

RESULTS AND DISCUSSION

I. Results for Planar Walking

The trajectory generation for the planar model of the humanoid was successfully completed. Figure 4 shows the movement of the base of the left leg with respect to the base of the right leg over the left cycle stages 1, 2, and 3. This figure is thus for the case where the left leg moves forward while the right leg is remaining as the stance leg. As recorded in Table 1 and shown in Figure 3 earlier, along the x-axis, the left foot starts at a position of -2 inches and ends at a position of 2. Similarly, along the z-axis, the left foot starts at a position of 0, rises to a height of 1 inch, and then falls back to 0. For the last stage, only the center of mass is shifted from one leg to the other leg. Thus, the position of the left leg with respect to the right leg remains constant while the center of mass linearly increases as shown in Figure 5. The movement of the right leg is symmetrical to that of the left leg. Hence, there was no need to generate separate trajectories for each leg.

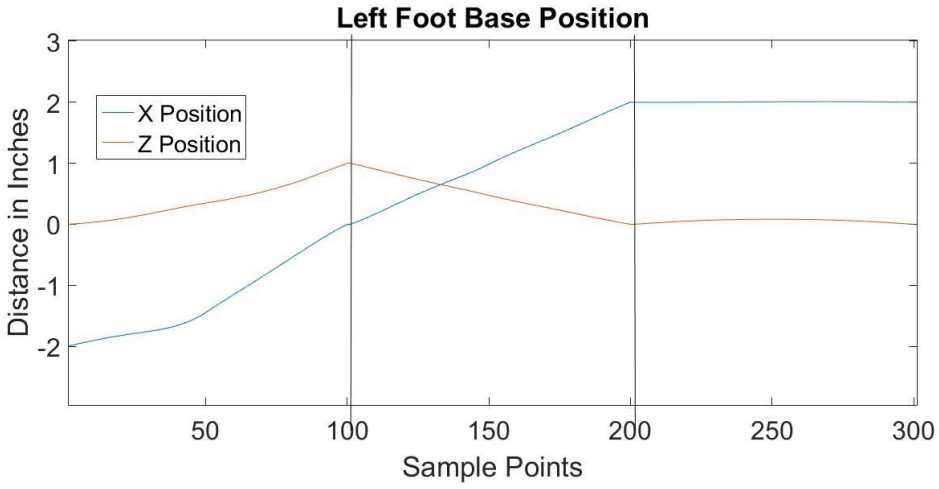

Figure 4: Change in left leg position along the x and z directions during Left Cycle Gait.

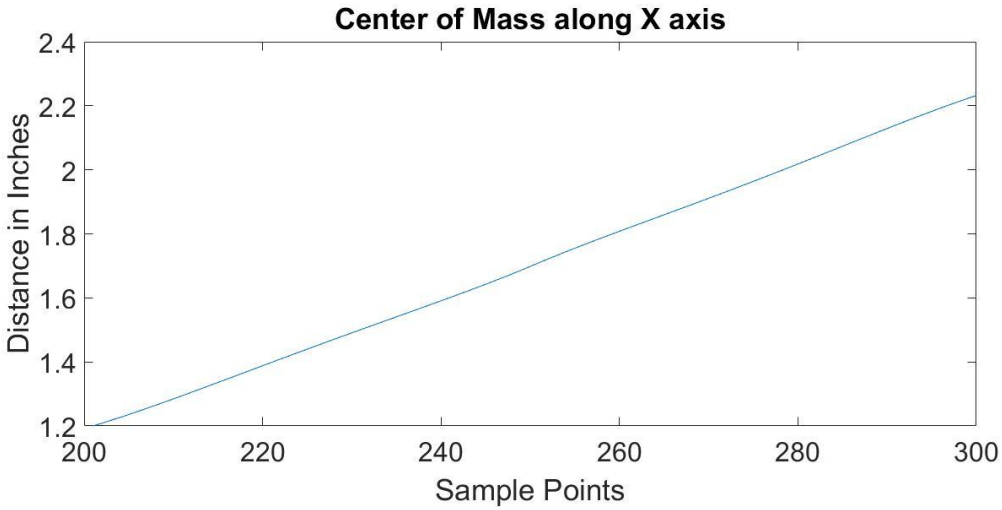

Figure 5: Change of center of mass position during Left Cycle Stage 3.

II. Results for 3D Walking Gait

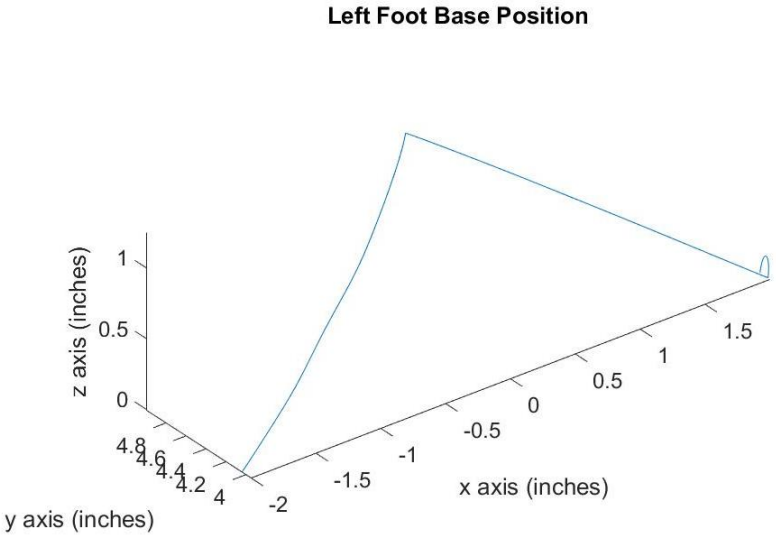

Figure 6: Change in left leg position along the x, y, and z directions during Left Leg Gait.

Following the method mentioned in section V of Chapter 2, the joint trajectories for a 3D walking gait was generated. Figure 6 shows the position of left foot base along all 3 axes during this left leg gait. Figure 7 shows the change in center of mass projection,

again along x, and y axes, during stage 3 of the walking gait. The end result of the gait synthesis was visualized using the 3D model of the robot in Matlab. The visualization of the left leg's motion and right leg's motion are displayed in Figures 8 and 9 respectively.

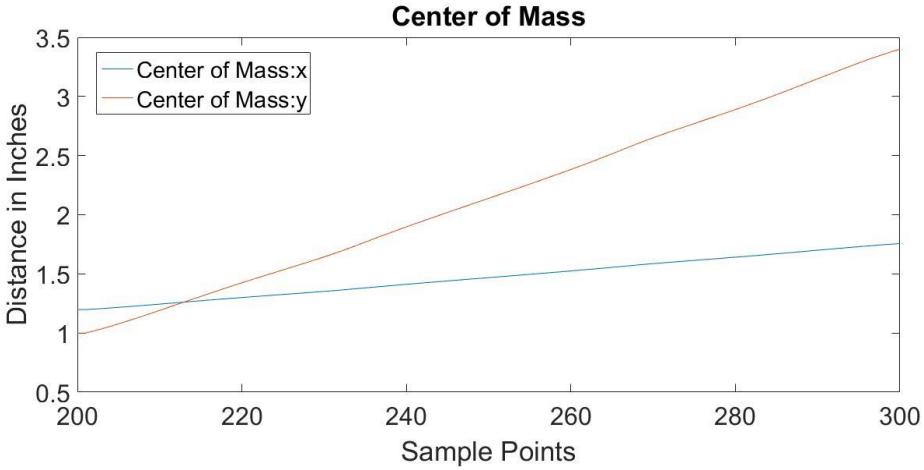

Figure 7: Change of center of mass position along x, and y directions during 3D Left Cycle Stage 3.

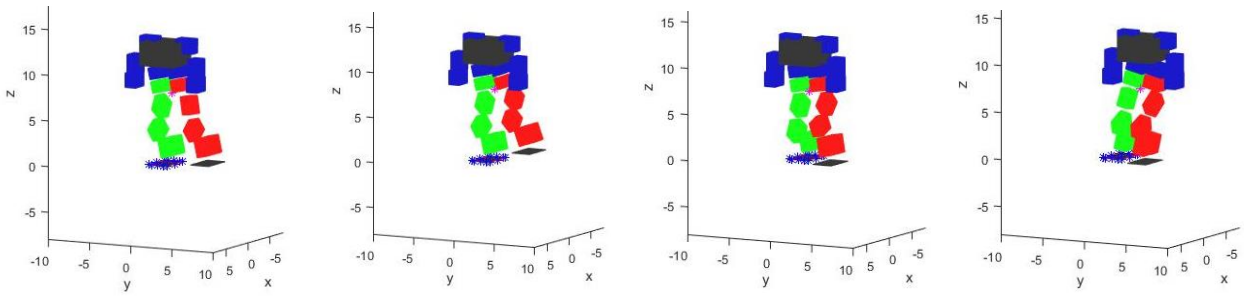

Figure 8. 3D left leg walking gait displayed on visual model in Matlab.

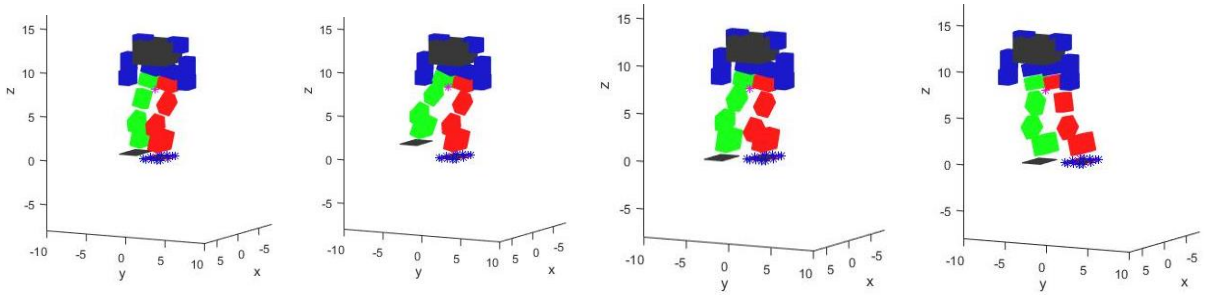

Figure 9. 3D right leg walking gait displayed on visual model in Matlab.

III. Discussion

The features of the trajectory generated can be analyzed to understand the success of trajectory generation using optimal control. The Pre-Cycle gait is required to set the right leg in front of the left leg. After this, as shown in Figure 3, Left-Cycle stage 1 of the gait is executed where the left leg of the robot is expected to move in z direction by a distance of 1 inch and in the x direction by a distance of 2 inches. Thus, at the end of this part of the gait the leg should have lifted up and forward while the projection of the center of mass must lie over the right leg. The requirement for a successful completion of this step is that the feet do not drag over the ground at any point. Hence, a constraint was added in the optimal control problem where an obstacle is avoided at the beginning of the gait. Figure 13 shows the result of the avoidance of this obstacle and thus the prevention of dragging of foot on the ground. This is important to reduce any unaccounted forces on the humanoid.

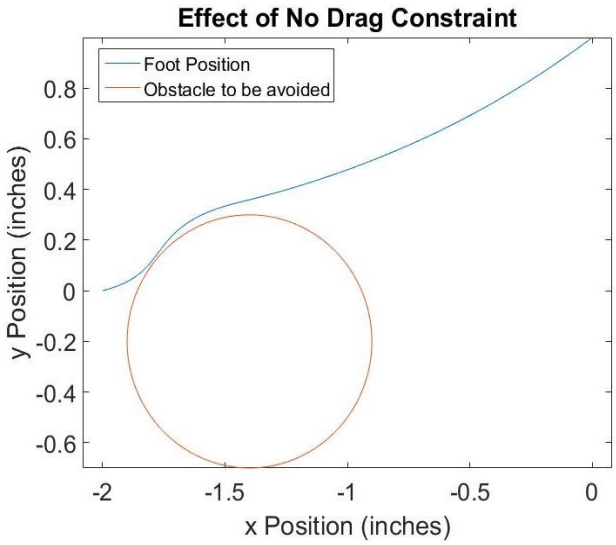

Figure 10: Obstacle Avoidance in Left Cycle Stage 1.

In left cycle stage 2, the left foot is expected to move forward by another 2 inches while slowly coming back to the ground. Thus z position should decrease while x position should increase. Again, while landing back on the ground any sort of drag must be avoided. In this case, the natural solution did not cause any drag. Therefore, no

obstacle avoidance condition was required. In the meantime, another very important constraint is that the feet do not try to push into the ground, as this would cause the body to become unstable. The results do satisfy all of the above requirements; the left leg position along the z axis does not go below 0.

The last part of the gait is the transition stage between moving left leg to moving right leg. During this stage, the center of mass needs to move in a way such that it is projected over the leg that does not move in the next part of the cycle. Thus in this particular case, the body must move in such a way that the center of mass is over the left leg at the end of the movement. Also, during this stage of the gait the two feet are expected to remain stationary on the ground. Figure 4 does show a slight discrepancy in the change of x position. But the change is so small that it does not cause any apparent error to the gait. As seen in Figure 5, at the end of this stage, the center of mass has shifted to the point 2.232 inches along the x axis, which is the region of the left leg foot. All the three stages mentioned above are shown in the biped visualization in Figure 3.

Since the right leg moves in a manner symmetric to the left leg, a repeat of the above process is unnecessary. Simply mirroring the joint angles successfully produced the joint angles required by the right leg to follow the same trajectory. Again, the execution of this trajectory on the visual model of the biped is shown in Figure 3 as well. Therefore, the optimal control problems set up as detailed in Section IV of Chapter 2 were able to generate a set of joint angles that could continuously be reused to allow the robot to walk in a cyclic manner. Since this is a planar model, the third dimension was supported by an external boom that could prevent the humanoid from falling along the y axis. The 3D walking gait generated also follows the same idea as above but with additions as

mentioned in Chapter 2 Section V. The trajectory generated satisfies all required constraints as mentioned in Tables 5, 6, and 7. Thus by setting up optimal control problems in terms of positions and center of mass of the body, both of which are functions of joint angles, we were able to generate the joint trajectories using Optragen and a solver.

IV. Future Work

Implementation of the 3D trajectories on the physical robot shows that the effect of the load on the stance foot prevents the robot from executing trajectories as seen in the visual model. The correction of this problem would require the implementation of an integral control that would balance the effect of the load on each motor. Once the 3D quasi-static walking is perfect, the next ideal step would be to generate dynamic walking gait for the humanoid. Dynamic walking is more energy efficient and similar to human walking. This step can also be achieved using the optimal control method explored in this thesis and would enable the robot to walk faster as well as improve efficiency.

REFERENCES

[1] J. Y. Kim, I. W. Park, J. Lee, M. S. Kim, B. K. Cho, and J. H. Oh, "System design and dynamic walking of humanoid robot KHR-2," *IEEE International Conference on Robotics and Automation*, pp. 1431-1436, 2005.

[2] C. Y. Q. Z. L. Xiao, "Walking stability of a humanoid robot based on Fictitious Zero-Moment Point "*International Conference on Control, Automation, Robotics and Vision*, pp. 1-6, 2006.

[3] A. Gams, J. van den Kieboom, F. Dzeladini, A. Ude, and A. J. Ijspeert, "Real-time full body motion imitation on the COMAN humanoid robot," *Robotica*, pp. 1049-1061, Jun 2015.

[4] J. Y. Kim, I. W. Park, and J. H. Oh, "Walking control algorithm of biped humanoid robot on uneven and inclined floor," *Journal of Intelligent & Robotic Systems*, pp. 457-484, Apr 2007.

[5] P. Michel, J. Chestnutt, J. Kuffner, and T. Kanade, "Vision-guided humanoid footstep planning for dynamic environments," *IEEE-RAS International Conference on Humanoid Robots*, pp. 13-18, 2005.

[6] J. P. Mattias Wahde, "A brief review of bipedal robotics research," *Mechatronics Forum International Conference*, pp. 480-488, 2002.

[7] S. Cotton, A. Murray, and P. Fraisse, "Statically equivalent serial chains for modeling the center of mass of humanoid robots," *IEEE-RAS International Conference on Humanoid Robots*, pp. 235-241, 2008.

[8] S. Kwon and Y. Oh, "Estimation of the center of mass of humanoid robot," *International Conference on Control, Automation and Systems*, pp. 2705-2709, 2007.

[9] S. Czarnetzki, S. Kerner, and O. Urbann, "Observer-based dynamic walking control for biped robots," *Robotics and Autonomous Systems*, pp. 839-845, Jul 31 2009.

[10] I. M. Motoc, K. Sirlantzis, S. Spurgeon, and P. Lee, "Zero moment point/inverted pendulum-based walking algorithm for the NAO Robot," *International Conference on Emerging Security Technologies*, pp. 63-66, 2014.

[11] J. Grizzle, G. Abba and F. Plestan, "Asymptotically stable walking for biped robots: analysis via systems with impulse effects", *IEEE Transactions on Automatic Control*, pp. 51-64, 2001.

[12] A. Ames, E.A. Cousineau and M.J. Powell, "Dynamically Stable Robotic Walking with NAO via Human-Inspired Hybrid Zero Dynamics", *Hybrid Systems, Computation and Control*, 2012.

[13] J. Yamaguchi, E. Soga, S. Inoue, and A. Takanishi, "Development of a bipedal humanoid robot - Control method of whole body cooperative dynamic biped walking," *IEEE International Conference on Robotics and Automation*, pp. 368-374, 1999.

[14]S. Hong, Y. Oh, B.-J. You, and S.-R. Oh, "A walking pattern generation method of humanoid robot MAHRU-R," *Intelligent Service Robotics*, pp. 161–171, Jun. 2009.

[15] S. Kajita, F. Kanehiro, K. Kaneko, K. Fujiwara, K. Yokoi, and H. Hirukawa, "A realtime pattern generator for biped walking," *IEEE International Conference on Robotics and Automation*, pp. 31-37, 2002.

[16] S. Hong, Y. Oh, D. Kim, and B.-J. You, "Real-time walking pattern generation method for humanoid robots by combining feedback and feedforward controller," *IEEE Transactions on Industrial Electronics*, pp. 355–364, 2014.

[17] A. Abdolmaleki, N. Shafii, L. P. Reis, N. Lau, J. Peters, and G. Neumann, "Omnidirectional walking with a compliant inverted pendulum model," *Advances in Artificial Intelligence*, pp. 481–493, 2014.

[18] J.-H. Kima, J. H. Choib, and B.-K. Choc, "Walking pattern generation for a biped walking robot using convolution sum," *Advanced Robotics*, no. 9-10, pp. 1115–1137, 2011.

[19] M. Khadiv, S. A. A. Moosavian, A. Yousefi-Koma, M. Sadedel, and S. Mansouri, "Optimal gait planning for humanoids with 3D structure walking on slippery surfaces," *Robotica*, pp. 1–19, Jan. 2015.

[20] Y. Luo, Z. Wu, S. Bi, Y. Zhang, Q. Zheng, and Q. Huang, "A biped humanoid robot's gait planning method based on Artificial Immune Network," *International Conference on Machine Learning and Cybernetics*, pp.292-297, 2014.

[21] C.Y. Chen, P.H. Huang, and W.C. Chou, "A critical review and improvement method on biped robot," *International Journal of Innovative Computing, Information, and Control*, pp. 5245–5254, Sep. 2011.

[22] O. Stasse and M. Bennewitz, "Guest editorial special issue on progress and open problems in motion planning and navigation for humanoids," *International Journal of Humanoid Robotics*, pp. 1402001-1402004, May 2014.

[23] Koch, Kai Henning, Katja Mombaur, and Philippe Soueres. "Optimization-Based Walking Generation For Humanoid Robot". *IFAC Proceedings Volumes* 45. pp. 498-504, 2012.

[24] R. Bhattacharya, "OPTRAGEN: A Matlab toolbox for optimal trajectory generation*," 45th IEEE Conference on Decision and Control*, p. 0191- 2216, 2006.

[25] Philip E. Gill , Walter Murray , Michael A. Saunders, “SNOPT: An SQP Algorithm for Large-Scale Constrained Optimization,” *SIAM Journal on Optimization*, p.979-1006, 2002

Acknowledgements

I am really grateful to Dr. Patricio Vela for providing me with such a great opportunity to conduct research under his guidance. I appreciate his continuous involvement in the project and it would have been impossible to complete the project without his dedication towards his students. I also thank Alexander Chang, my graduate mentor, for his patience and support. I would like to mention my gratitude towards Dr. Erik Verriest for being my faculty advisor and providing meaningful feedback. Lastly, I thank Siddharth Mehta for being a supportive and great teammate.